Journal of *Marine Science and Engineering*

MDPI

Article

Seasonal Temperature and Nutrient Fluctuations Reshape Phytoplankton Assembly and Network Vulnerability in a Coastal Ecosystem

Haolei Shi [1], Jiantao Cao [1], Fajin Chen [2], Peng Wang [1] and Guodong Jia [1,3,*]

[1] State Key Laboratory of Marine Geology, Tongji University, Shanghai 200092, China
[2] College of Ocean and Meteorology, Guangdong Ocean University, Zhanjiang 524088, China
[3] Southern Marine Science and Engineering Guangdong Laboratory (Zhuhai), Zhuhai 519082, China
* Correspondence: jiagd@tongji.edu.cn

Abstract

Temperature and nutrient availability are pivotal drivers of coastal phytoplankton dynamics; however, how they regulate the interplay between community assembly and ecological network stability remains less explored. In this study, we integrated 18S rRNA high-throughput sequencing with molecular ecological network analysis and the iCAMP model to investigate the seasonal succession and driving mechanisms of phytoplankton in a coastal region (Qiongdong) of the South China Sea. Our results suggest that water temperature is a key factor influencing community succession. However, rather than following a linear response to temperature rise, the molecular ecological network exhibited a significant network contraction in spring, characterized by minimized complexity and peak vulnerability. This structural shift coincided with a transition in nutrient limitation (from phosphorus to nitrogen) induced by spring upwelling. Assembly process analysis revealed that while stochastic processes dominated overall community construction, a notable increase in dispersal limitation occurred in spring. The intensification of dispersal limitation driven by changes in the nutritional structure may be the main cause of network simplification and reduced stability. In conclusion, our findings highlight that while temperature affects the seasonal replacement of phytoplankton species, nutrient-induced shifts in assembly mechanisms degrade ecological network integrity in coastal environments.

Keywords: phytoplankton; molecular ecological network; assembly process; 18S rRNA; Qiongdong

Check for updates

Academic Editor: Sang Heon Lee

Received: 24 March 2026
Revised: 7 April 2026
Accepted: 8 April 2026
Published: 10 April 2026

Copyright: © 2026 by the authors. Licensee MDPI, Basel, Switzerland. This article is an open access article distributed under the terms and conditions of the Creative Commons Attribution (CC BY) license.

1. Introduction

As primary producers in marine ecosystems [1], phytoplankton play a fundamental role in carbon fixation and energy transfer, thereby supporting marine food webs and driving global biogeochemical cycles [2,3]. Temperature and nutrients are key drivers of phytoplankton community succession [4–6]. However, across distinct seasonal environmental gradients, the specific mechanisms by which the co-variation in these environmental factors reshapes the phytoplankton community still require further investigation.

Compared with traditional species-based analyses, molecular ecological networks (MENs) analysis provides a powerful framework for inferring potential interactions among eukaryotic plankton taxa [7,8]. An increasing number of studies have applied MENs to eukaryotic phytoplankton communities to explore the impact of environmental changes on the complexity and stability of phytoplankton networks [9–11]. Notably, in coastal

ecosystems, temperature and nutrient conditions often change in an intertwined manner under the influence of monsoons, which makes the response mechanism of eukaryotic phytoplankton networks more complex. Whether the changes in phytoplankton molecular ecological networks are mainly driven by physiological and metabolic responses to temperature or by structural reorganization resulting from alterations in nutrient structure remains to be further clarified. Clarifying this issue is of great significance for understanding the adaptive mechanisms of phytoplankton communities to environmental changes.

The community structure of eukaryotic phytoplankton is shaped not only by species interactions but also by underlying assembly processes [12–15]. Ecological theory typically divides the processes of community assembly into deterministic processes and stochastic processes [12]. Deterministic processes (i.e., environmental filtering) are generally considered the primary drivers of community dynamics [16] and are mainly categorized into heterogeneous selection and homogeneous selection. Heterogeneous selection promotes community divergence under varying environmental conditions, leading to high β-diversity, whereas homogeneous selection results in community convergence under similar conditions, reducing β-diversity [17]. In contrast, stochastic processes-such as dispersal limitation and ecological drift-introduce randomness into community dynamics [13]. Although community assembly processes and ecological network integration have received increasing attention in the study of eukaryotic phytoplankton communities [7,9,18], there is still a lack of systematic research on coupling assembly mechanisms with network stability to explain, from a mechanistic perspective, how seasonal environmental gradients drive the collapse or reinforcement of phytoplankton interactions in coastal areas influenced by upwelling.

The sea area east of Hainan Island (the Qiongdong region) in the northwestern South China Sea is a typical coastal ecosystem strongly influenced by monsoon dynamics. During summer, the southwest monsoon induces pronounced coastal upwelling (April–September, peaking from June to August), which brings cold, nutrient-rich subsurface waters to the surface [19]. In winter, the northeast monsoon drives the southward transport of cold waters along the coast, leading to lower sea surface temperatures in the northern region [20]. These processes driven by the monsoon result in strong seasonal gradients in temperature and nutrient conditions, which greatly alter the composition of microbial communities [21,22]. However, changes in species composition or diversity alone may not fully capture how communities respond to environmental fluctuations.

In this study, we employed 18S rRNA high-throughput sequencing to characterize phytoplankton communities in the Qiongdong region across different seasons. By integrating MENs with the iCAMP model, we aimed to: (1) characterize the seasonal succession of phytoplankton under varying temperature and nutrient gradients; (2) identify the key environmental drivers underlying shifts in ecological network complexity and robustness; (3) elucidate how community assembly processes influence the complexity and stability of these networks. Our findings provide new mechanistic insights into the maintenance of coastal phytoplankton diversity and the resilience of marine ecosystems in a changing environment.

2. Methods

2.1. Samples and Pretreatment

Surface seawater samples (0–2 m) were collected from the Qiongdong region across three discrete sampling periods (Figure 1), which represent the seasonal hydrological stages driven by monsoon in the Qiongdong region: May 2024 (QD5, spring, generally regarded as the beginning of the Qiongdong upwelling driven by the southwest monsoon), August 2024 (QD8, summer, typically considered the peak period of the Qiongdong upwelling driven

by the southwest monsoon), and February 2025 (QD2, winter, when the northeast monsoon prevails without upwelling). At each of the 25 sites per period, 6 L of seawater were collected. The seawater was filtered through 47 mm diameter polycarbonate membranes (0.45 μm pore size, Merck Millipore) using a vacuum pump (GM-0.333A, Tianjin Jinteng Experiment Equipment Co., Ltd., Tianjin, China) to obtain suspended particulates. Particulates were stored at −20 °C until further processing in the laboratory. The full-depth profiles of temperature and salinity were measured using a calibrated SBE 911plus CTD device (Sea-Bird Electronics, Inc., Bellevue, WA, USA). Nutrients (NO^{2-}+NO^{3-}, NH^{4+}, PO_4^{3-}, and SiO_3^{2-}) were determined using a San++ continuous flow analyzer (Skalar, Breda, The Netherlands). The detection limits for NO^{2-}+NO^{3-}, NH^{4+}, PO_4^{3-}, and SiO_3^{2-} were 0.1 μmol L^{-1}, 0.1 μmol L^{-1}, 0.02 μmol L^{-1}, and 0.45 μmol L^{-1}, respectively.

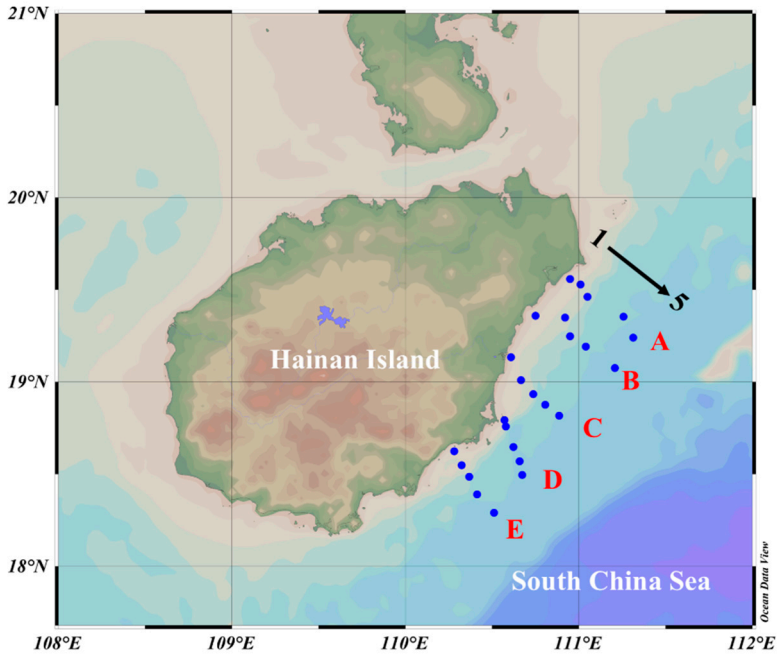


Figure 1. Distribution map of sampling stations in the Qiongdong region. Five sections (A–E) were established along the coast of the study area, with each section containing five sampling stations. Black arrows indicate the station numbering sequence from nearshore to offshore (Stations 1–5). Samples were collected at these 25 stations during three distinct periods: May 2024 (QD5), August 2024 (QD8), and February 2025 (QD2).

2.2. DNA Extraction and Quantitative PCR

The genomic DNA of microorganisms in the surface seawater was extracted using MOBIO's PowerWater® DNA Isolation Kit. The abundance of 18S rDNA was quantified using the Hangzhou Borui FQD-96A fluorescence quantitative PCR instrument (Hangzhou, China). The 18S primers were 565F (CCAGCASCYGCGGTAATTCC) and 981R (ACTTTCGTTCTTGATYRATGA) [23].

2.3. Library Construction and Sequencing

The 18S rRNA gene in the 18S V4 region was amplified to identify eukaryotic microbial diversity. The 18S primers were 565F and 981R [23]. Library construction was performed according to the standard procedure of NEBNext® Ultra™ II DNA Library Prep Kit for Illumina® (New England Biolabs, Ipswich, MA, USA). After quality control, amplicon libraries were sequenced (PE250) on the Illumina Nova 6000 platform by Guangdong Magigene Biotechnology Co., Ltd. (Guangzhou, China).

2.4. Sequencing Data Processing

The raw sequences were subjected to sliding window quality control (window 50bp, average quality Q20) by fastp (v0.14.1) [24], and then the primers were removed by cutadapt to obtain Clean Reads. Usearch-fastq_mergepairs (V10) was used to concatenate the two ends of sequences to obtain Raw Tags, and fastp was used for secondary quality control to obtain Clean Tags. The RDP Naive Bayes classifier, integrated within the DADA2 pipeline, was employed to classify Amplicon Sequence Variants (ASVs) [25]. The representative sequence of each ASV was compared against the SILVA 132 database for taxonomic annotation [26], with a confidence threshold set at 0.8.

2.5. Statistical Analysis

The classification annotations were verified based on the AlgaeBase (www.algaebase.org, accessed on 1 February 2025) and NCBI databases to screen for phytoplankton amplicon sequence variants (ASVs). Additionally, non-target groups (including those belonging to the Rhizaria, Animalia, Amoebozoa, Centrohelida, Discoba, Fungi, and "unclassified" and other non-planktonic plant ASVs) were excluded [27]. The relative abundance of phytoplankton at the phylum level in each sample was calculated as the proportion of ASV sequences of the same taxonomic group to the total phytoplankton sequences [27]. The total eukaryotic copy number was quantified by 18S rRNA primer qPCR, and a gene-copy-based proxy for absolute abundance was estimated by multiplying the total copy number by the relative abundance [28]. Although this study focuses predominantly on eukaryotic phytoplankton, 18S rRNA sequences assigned to Metazoa were separately quantified. The proportion of Metazoa sequences relative to the total 18S rRNA pool was subsequently analyzed to evaluate potential ecological interactions between Metazoa and the phytoplankton community.

The obtained phytoplankton data were statistically analyzed as follows: (1) Alpha diversity indices (Richness, Pielou evenness, Shannon, and Simpson) were calculated based on ASV abundance tables using the R package vegan [21], and differences among groups were tested by ANOVA. (2) Based on the ASV abundance table, the bray_curtis distance algorithm in the vegan package of R (version 4.5.0) was used to analyze the NMDS (Non-metric multidimensional scaling) analysis [29]. Differences in community structure were further evaluated using ANOSIM. (3) CCA (Canonical Correspondence Analysis) was conducted based on ASV classification level and environmental factor data [30].

2.6. Molecular Ecological Network Analysis

Based on the pairwise correlations of ASV abundances, a molecular ecological network was constructed using the integrated network analysis pipeline (iNAP) [31]. First, low-abundance taxa—defined as ASVs detected in less than 80% of all samples—were filtered out to reduce sparsity and improve the reliability of correlation estimates. Spearman's correlation coefficients were calculated for all pairwise ASVs. To avoid arbitrary threshold selection and reduce false correlations, a data-driven similarity threshold (0.83) was determined based on random matrix theory (RMT). Only correlations exceeding this RMT-derived threshold were retained to generate the adjacency matrix, and isolated nodes were subsequently removed. Network visualization was conducted using Gephi version 0.9.2, and the topological features of the network were calculated [32].

Key taxa were identified based on their topological roles through within-module connectivity (Zi) and between-module connectivity (Pi). Nodes were classified as module hubs ($Zi \geq 2.5$), connectors ($Pi \geq 0.62$), or network hubs ($Zi \geq 2.5$ and $Pi \geq 0.62$) [9].

Network stability assessment: Network stability is evaluated using robustness and vulnerability indicators. Robustness is determined through two simulated extinction exper-

iments: (I) Random robustness: calculate the proportion of remaining nodes after randomly removing 50% of the taxonomic units; (II) Targeted robustness: calculate the proportion of remaining nodes after removing three module hubs. Vulnerability is measured by the maximum decline in global efficiency after removing a single node, reflecting the network's dependence on key nodes.

2.7. Community Assembly Analysis

The assembly processes of phytoplankton communities across different seasons were analyzed using the Sloan Neutral community model (NCM) [33] and the iCAMP model [34]. NCM used the R package "minpack.lm" for model fitting, and the confidence interval and statistical analysis calculations were performed using the "Hmisc" and "stats4" packages. iCAMP was analyzed using the R packages "ape" and "iCAMP", utilizing the β nearest taxon index (βNRI) as the core metric, integrated with a modified Raup-Crick (RC) index to quantify the relative contributions of specific community assembly processes [12].

3. Results

3.1. Seasonal Environmental Heterogeneity

The temperature in the Qiongdong region shows obvious spatial variations in both horizontal and vertical distributions (Figure 2). Horizontally, the distribution of sea surface temperature (SST) showed a consistent nearshore-offshore gradient in all three seasons. Vertically, for example, transect C showed significant seasonal variations in the temperature profile. In winter (QD2), nearshore SST was lower than the subsurface temperature, together with the horizontal SST distribution, indicating a northerly alongshore current driven by the prevailing northeast wind. In spring (QD5), an active coastal upwelling induced by the southwest wind was evident, with uniform vertical temperature. In summer (QD8), although a southwest wind prevailed, upwelling was not evident during our sampling period, and a distinct thermal stratification was observed, likely due to a significant rise in surface temperature under intense sunlight. Isotherms ranging from 25 °C to 27.5 °C were densely distributed at depths of 20–40 m, forming a distinct thermocline.

Temporally, sea surface environmental factors in the Qiongdong region also showed obvious seasonal variations (Figure 3), among which SST is identified as the most active variable ($p < 0.001$). One-way ANOVA analysis showed that SST varied significantly among seasons ($p < 0.001$) (Figure 3). SSTs were lowest in winter, averaging 21.79 °C (range: 18.73–23.65 °C). They rose in spring to an average of 25.50 °C (range: 22.60–28.00 °C), and peaked in summer at 29.51 °C on average (range: 26.54–30.94 °C). Seasonal salinity variation was minimal due to the small input of freshwater from Hainan Island. For nutrients, dissolved inorganic nitrogen (DIN) was highest in spring (0.97 μmol L^{-1} on average), followed by winter (0.80 μmol L^{-1}) and summer (0.57 μmol L^{-1}), with no significant seasonal differences among the three seasons ($p = 0.1667$; Figure 3). Phosphate (PO_4^{3-}) showed the most pronounced variation: it was extremely low in winter (mean 0.002 μmol L^{-1}, with 20 sites below detection) but increased sharply in spring to 0.21 μmol L^{-1} (range: 0.12–0.30 μmol L^{-1}), detected at all stations. In summer, it declined again to 0.014 μmol L^{-1} (range: 0–0.13 μmol L^{-1}). Phosphate in spring was significantly higher than in winter and summer ($p < 0.001$; Figure 3). Silicate (SiO_3^{2-}) averaged highest in summer (3.34 μmol L^{-1}), significantly exceeding spring (2.03 μmol L^{-1}) and winter (1.67 μmol L^{-1}) levels ($p < 0.001$; Figure 3). Overall, nutrient dynamics were characterized by a distinct phosphorus (PO_4^{3-}) pulse in spring when an active upwelling occurred (Figure 2), shifting the system from P-limitation (winter/summer, N/P > 16) to N-limitation (spring, N/P = 4.68 ± 2.21).

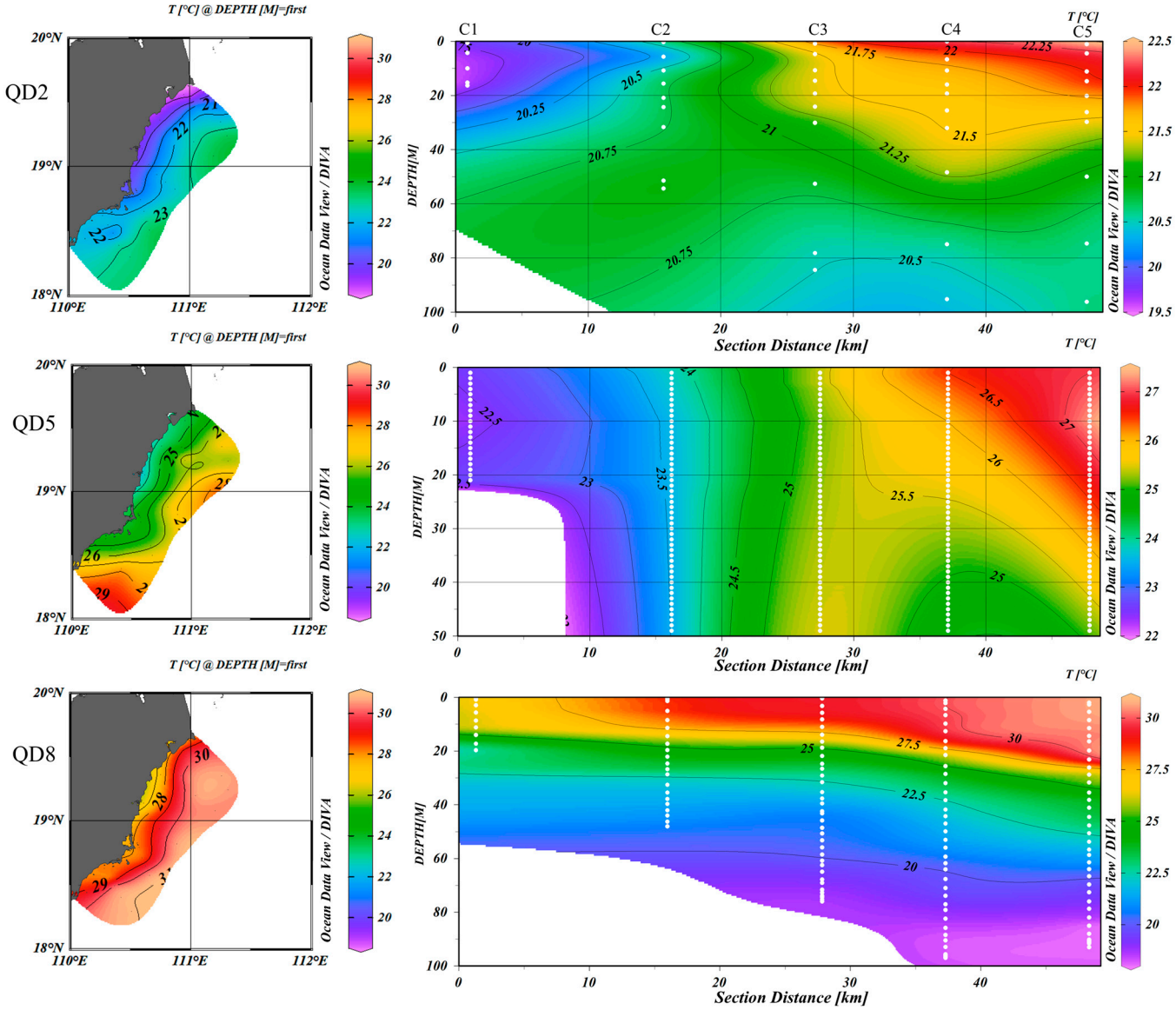


Figure 2. Spatiotemporal distribution of seawater temperature in the Qiongdong region. The three left panels show the horizontal distribution of surface seawater temperature in winter (QD2), spring (QD5), and summer (QD8). The three right panels present the vertical temperature profiles of section C (stations C1–C5). The black solid lines represent isotherms, with the values in degrees Celsius (°C).

3.2. Phytoplankton Succession and Diversity Shifts

Phytoplankton community structure shifted markedly across seasons, closely tied to environmental gradients. NMDS analysis revealed that the communities formed distinct, seasonally segregated clusters (Figure 4a), indicating substantial compositional differences between seasons. This seasonal differentiation was statistically confirmed by ANOSIM, which yielded moderately high R values ranging from 0.55 to 0.84 (p = 0.001, Table S1). These results demonstrate that differences between seasons were significantly greater than variations among spatially distributed samples within the same season.

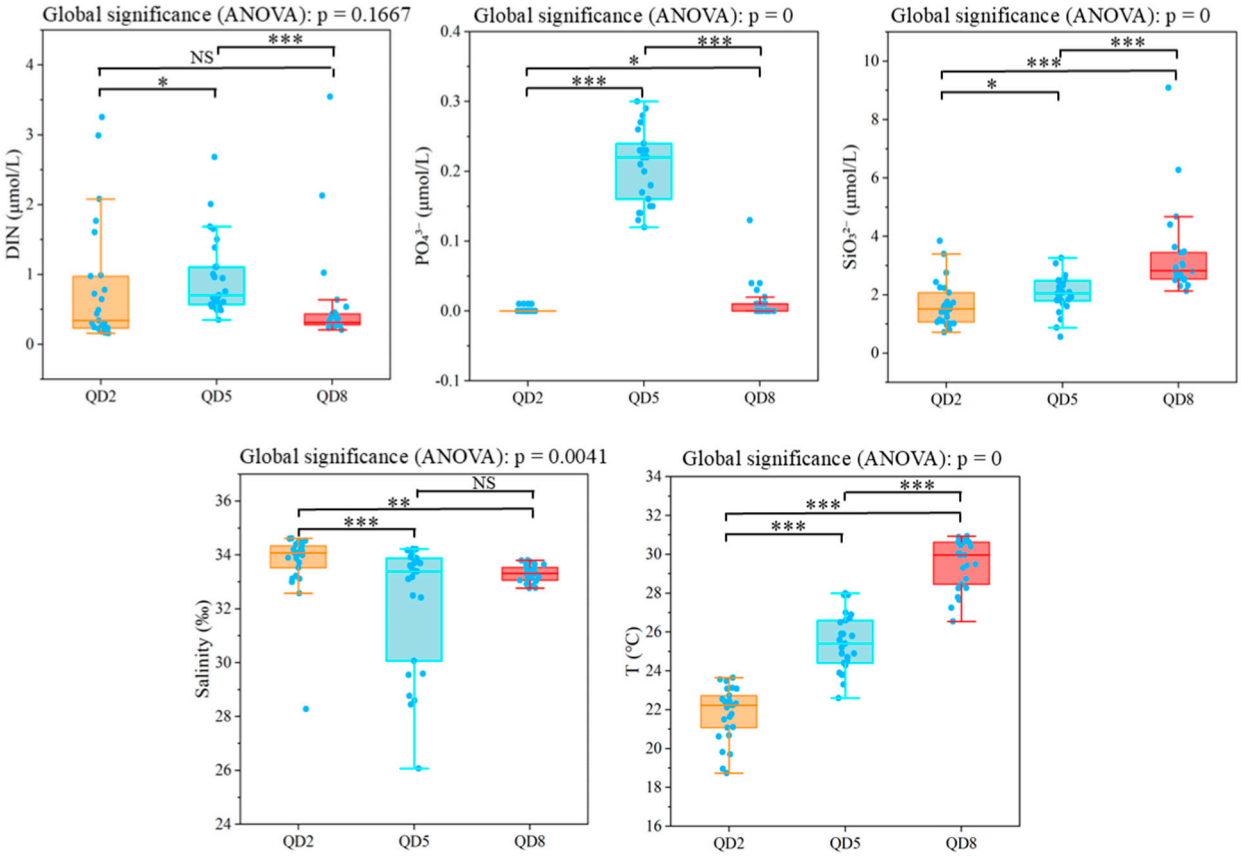


Figure 3. Box plots of environmental factors in three seasons. The box represents the interquartile range, the middle line represents the median, and the whiskers represent the minimum and maximum values. QD2: winter; QD5: spring; QD8: summer. The one-way ANOVA was used to test differences among seasons. NS indicates no significant difference, * $p < 0.05$, ** $p < 0.01$, *** $p < 0.001$.

The CCA results showed that the first two ordination axes together explained 65.4% of the total community variation (Figure 4b), suggesting that they captured most of the environmentally driven changes in the community. Among all measured factors, temperature had the longest vector in the CCA biplot, identifying it as the most influential environmental variable and the key driver of phytoplankton succession. Furthermore, temperature was significantly correlated with the NMDS ordination axes (Figure S1), providing additional, independent support for its central role in structuring the community seasonally.

Community composition shifted markedly with the seasons, aligning with the temperature gradient (Figure 4c). In winter, the community was mainly dominated by Dinoflagellata and Chlorophyta. During spring, the relative abundance of Bacillariophyta (diatom) and Dinoflagellata increased, whereas Chlorophyta declined. In summer, Ochrophyta reached its highest proportion while Chlorophyta decreased further. The gene-copy-based proxy for absolute phytoplankton abundance declined from winter to summer, indicating reduced total phytoplankton biomass (Figure S2). In contrast, α-diversity increased with seasonal temperature, as reflected by higher Shannon and Simpson indices in warmer seasons (Figure S3). These patterns collectively suggest a seasonal transition from the dominance by a few taxa toward a more even community structure along the seasonal temperature gradient.

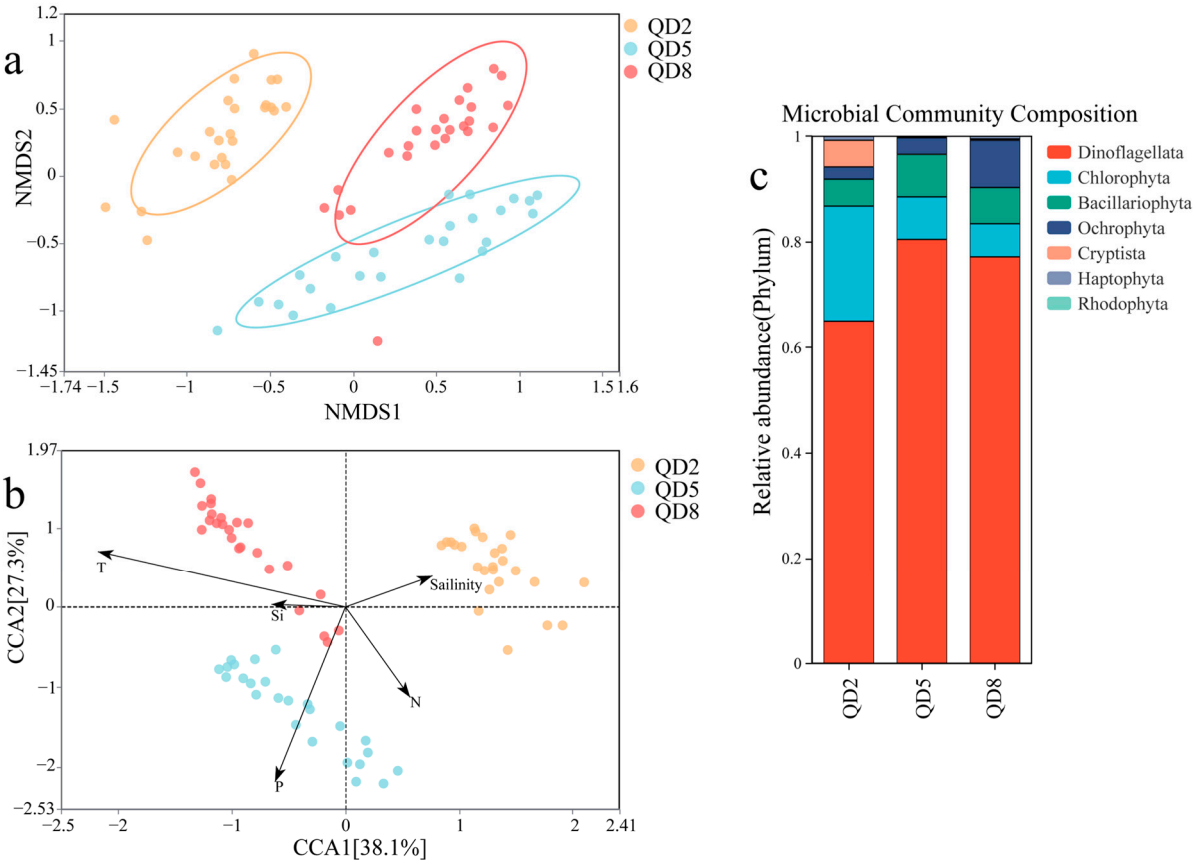


Figure 4. Seasonal variation in phytoplankton community structure and its relationship with environmental factors in the Qiongdong region. (**a**): NMDS ordination of phytoplankton communities at the ASV level based on Bray–Curtis distance, showing seasonal clustering patterns. (**b**): CCA showing the relationships between phytoplankton community composition (ASV level) and environmental variables. Arrows indicate the direction and strength of environmental gradients, with longer arrows representing stronger explanatory power. (**c**): Relative abundance of phytoplankton communities at the phylum level across seasons. QD2: winter; QD5: spring; QD8: summer.

3.3. Network Contraction and Vulnerability

Network topology analysis revealed a nonlinear pattern in the molecular ecological network across seasons (Figure 5). In winter, the network exhibited the highest structural complexity, characterized by a greater number of nodes and edges, a higher average degree, and stronger connectivity (Figure 6a–d). The network contained more module hubs, network hubs, and connectors, reflecting a more interconnected structure (Figure 7).

In spring, the network showed a marked contraction, with substantial decreases in node number, edge number, average degree, and overall connectivity (Figure 6a–d). Most nodes were classified as peripheral nodes, while module hubs and network hubs were rarely observed (Figure 7). Network vulnerability reached its highest level during this period (Figure 6i).

In summer, the network partially recovered, with increases in the number of nodes and edges, and the reappearance of several module hubs (e.g., ASV6 and ASV66) (Figures 6a,b and 7). However, the proportion of negative correlations increased compared to winter (Figure 6f). Meanwhile, network robustness decreased progressively from winter to summer, reaching the lowest level in summer (Figure 6g–h).

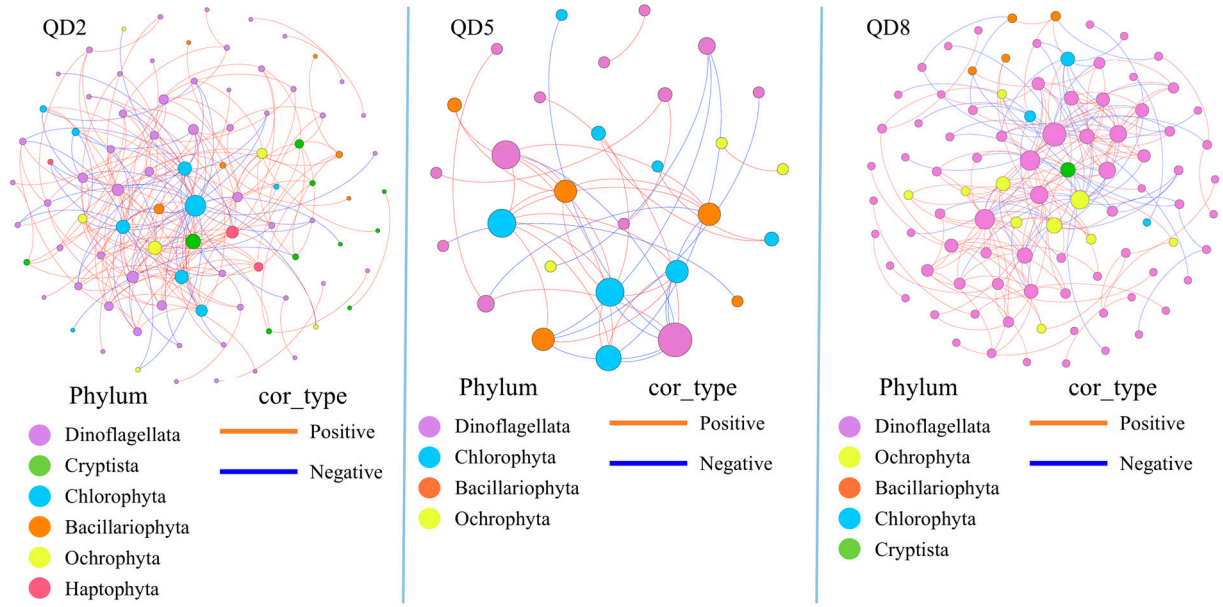


Figure 5. Molecular ecological network structure of phytoplankton. Nodes represent ASVs, and edges indicate significant correlations between species ($p < 0.05$). Red edges represent positive correlations, and blue edges represent negative correlations. Node size is proportional to node degree (degree). QD2: winter; QD5: spring; QD8: summer.

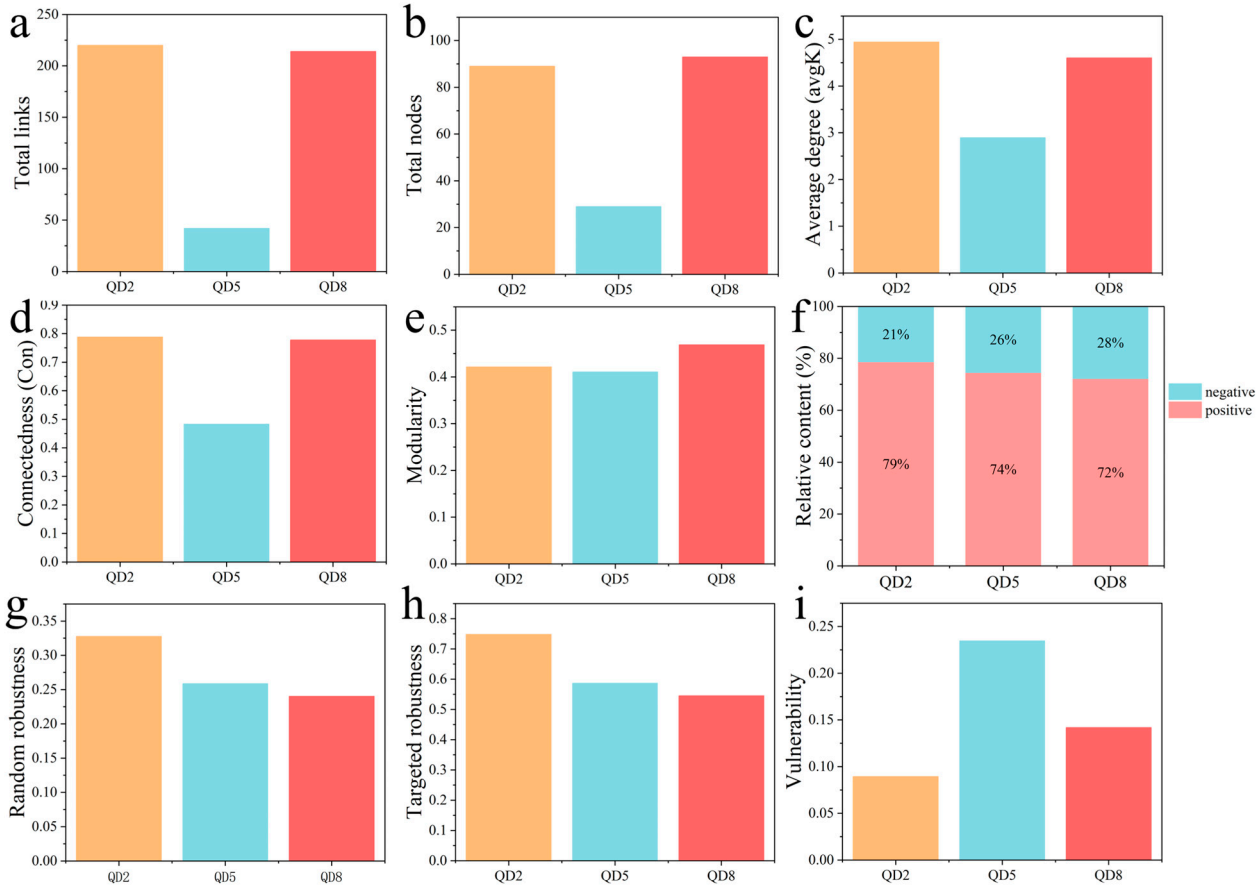


Figure 6. (**a**–**f**): Bar chart of topological parameters of co-occurrence networks of phytoplankton in different seasons. (**g**–**i**): Robustness and vulnerability analysis of the molecular ecological network of phytoplankton in different seasons. QD2: winter; QD5: spring; QD8: summer.

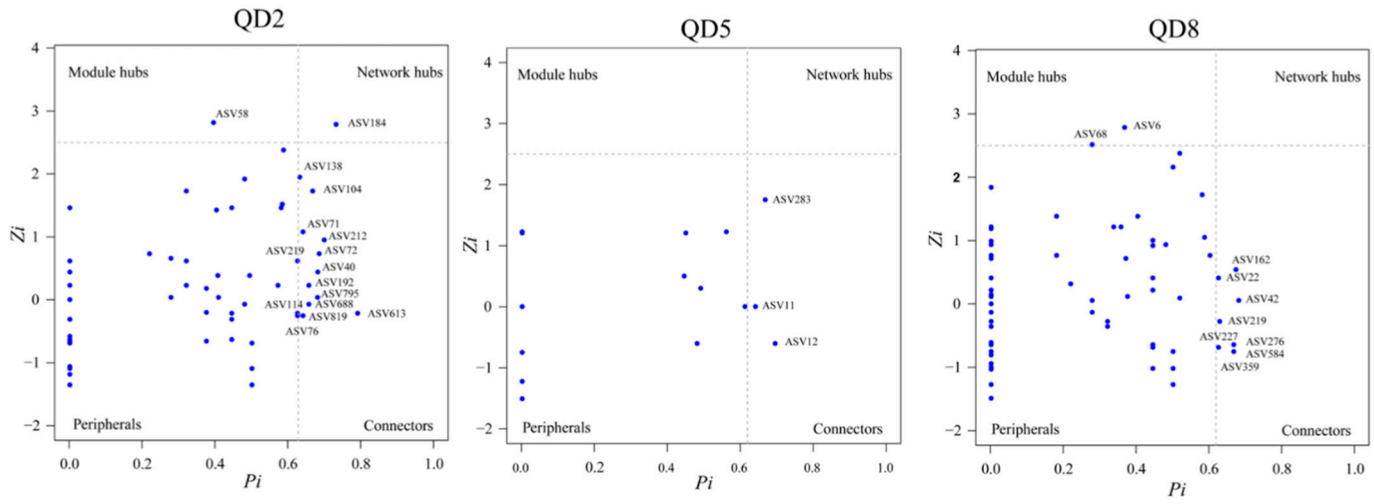


Figure 7. Node role classification based on Zi-Pi analysis. Zi represents the intra-module connection degree of a node, and Pi represents the inter-module connection degree. Nodes are classified as peripherals, connectors, module hubs, and network hubs based on the thresholds of Zi and Pi. QD2: winter; QD5: spring; QD8: summer.

3.4. Assembly Processes and Dispersal Limitation

To reveal the mechanisms of phytoplankton community assembly in the Qiongdong region during different seasons, this study combined the neutral community model (NCM) with the iCAMP null model for analysis. The NCM results (Figure 8) indicated that phytoplankton communities across all seasons could be well fit by the neutral model ($R^2 > 0.65$), suggesting that stochastic processes played a significant role in community assembly. However, R^2 varies with the seasons, reaching its lowest point in spring (QD5), which is lower than that in winter (QD2) and summer (QD8). Notably, the migration rate (m) also shows a similar seasonal trend, dropping from 0.0082 in winter to 0.0033 in spring, and then rising to 0.0074 in summer. This decline indicates a substantial reduction in species dispersal and spatial connectivity among communities during spring.

Based on this, the iCAMP analysis further quantitatively dissected the community assembly process (Figure 9). iCAMP quantitatively divides the community assembly process into deterministic processes (heterogeneous selection + homogeneous selection) and stochastic processes (dispersal limitation + homogeneous dispersal + drift). Overall, the proportion of random processes exceeded 50% in all three seasons, indicating that random mechanisms dominated community assembly (Figure 9a). However, at the specific mechanism level, homogeneous selection (HoS), a deterministic process, was the most powerful single driver, with a relatively stable proportion in each season (44–46%) (Figure 9b), reflecting the continuous environmental filtering effect in this sea area. Notably, in spring (QD5), a distinct structural shift occurred within the stochastic process (Figure 9b). The contribution of dispersal limitation (DL) increased, while drift (DR) correspondingly decreased. This finding is highly consistent with the decline in the m value in NCM, jointly confirming that dispersal limitation is enhanced during this spring period.

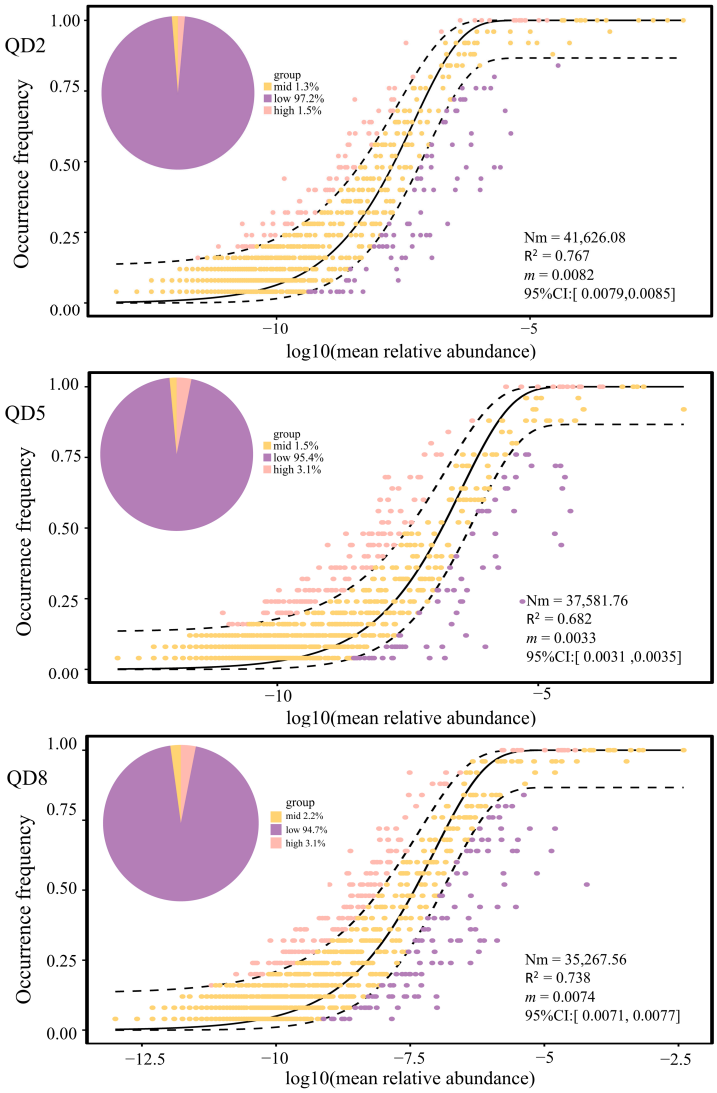


Figure 8. Fitting results of the neutral community model (NCM). The x-axis represents the occurrence frequency of ASVs, and the y-axis represents the relative abundance. The solid line indicates the model fitting result, and the dashed line indicates the 95% confidence interval. R^2 represents the goodness of fit. m indicates the migration rate.

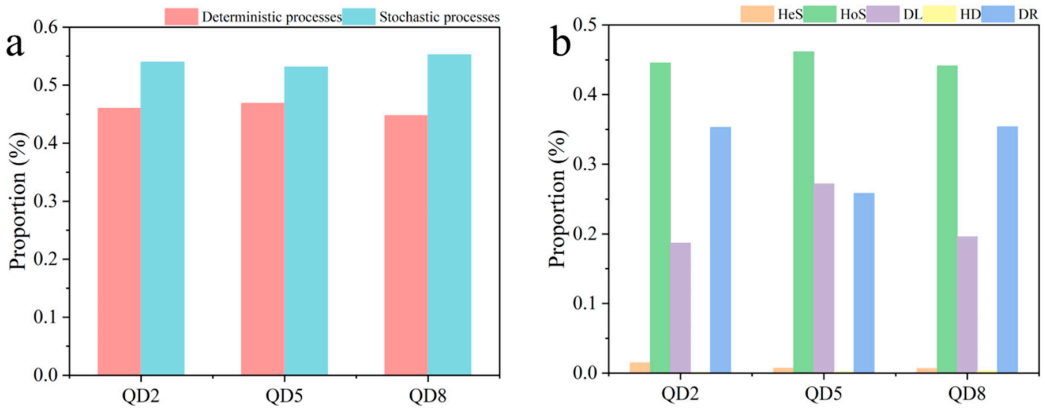


Figure 9. Relative contributions of community assembly processes inferred based on the iCAMP model. (**a**): The proportion of deterministic processes (the sum of heterogeneous selection [HeS] and homogeneous selection [HoS]) and stochastic processes (the sum of dispersal limitation [DL], homogeneous dispersal [HD], and drift [DR]). (**b**): Detailed contribution proportions of each specific ecological process. QD2: winter; QD5: spring; QD8: summer.

4. Discussion

4.1. Seasonal Upwelling-Driven Reconstruction of Nutrient Structure

Seasonal variations in the temperature structure and nutrient levels in the Qiongdong region are closely related to the Qiongdong upwelling process. In winter, under the influence of the East Asian monsoon, the cold-water mass from the north invades the area [20], resulting in a phenomenon where the bottom water is warm, the surface water is cold near the shore, and the nutrient content in the sea is relatively low. May in spring is generally the period when the Qiongdong upwelling begins [19]. The isotherms near the shore rise sharply and tend to be vertically distributed, indicating a significant increase in vertical transport and mixing of the water body. The upwelling brings nutrient-rich subsurface water to the surface [21], leading to a synchronous increase in nutrients. At the same time, PO_4^{3-} is positively correlated with salinity ($R^2 = 0.47$), indicating that they mainly originate from the high-salinity upwelling water rather than from land-based inputs. In contrast, although summer is traditionally regarded as the peak period of upwelling [19], the intense warming of the surface layer leads to strong thermal stratification, forming a natural physical barrier that effectively hinders the penetration of deep cold water to the surface and weakens the vertical exchange efficiency [35]. Therefore, the vertical supply of nutrients to the surface layer by upwelling in spring makes spring the turning point when nutrients in the Qiongdong region shift from scarcity to abundance.

It is worth noting that the overall concentration of nutrients in spring increased, and the N/P ratio underwent a significant change. The N/P ratio dropped below the Redfield ratio (16:1), indicating that the system shifted from phosphorus limitation to nitrogen limitation [36]. This low N/P feature may be modulated by large-scale water mass transport. The Kuroshio Branch, originating from the western Pacific, brings the western Pacific water mass with low N/P characteristics [37] into the northern South China Sea through the Luzon Strait, and its upper 300 m water layer advances westward along the continental slope of the Chinese mainland [38]. Therefore, the spring upwelling not only transports nutrient-rich subsurface water to the surface but also brings the low N/P signal into the nearshore surface water, promoting a shift in the nutrient structure from phosphorus limitation to nitrogen limitation. Such a shift may become an important mechanism driving the seasonal succession of phytoplankton community structure, as discussed below.

4.2. Environmental Controls on Seasonal Phytoplankton Community Structure

Seasonal changes in phytoplankton communities in coastal complex ecosystems are the result of the interactions among multiple environmental factors [5,6,39,40]. This study reveals that in the Qiongdong region, water temperature is a key factor influencing seasonal community changes. The NMDS ordination axes are significantly correlated with temperature, indicating that the temperature gradient dominates the seasonal differentiation of the community structure. Temperature not only directly regulates the metabolic rate and photosynthetic efficiency of phytoplankton [41], but also influences their resource utilization efficiency through interactions with other environmental factors [42,43]. As seasonal temperature increases, the α diversity (Shannon and Simpson indices) increases, suggesting that seasonal temperature rises may enhance the competitiveness of specific functional types of phytoplankton, thereby affecting the community structure and ecological function [43].

It should be noted that, although α diversity increased, the gene-copy-based abundance proxy (as a surrogate for absolute abundance) of phytoplankton decreased with the seasonal increase in temperature. Research has found that an increase in temperature enhances the feeding activity of zooplankton, thereby reducing the absolute abundance of

phytoplankton [44]. In this study, the relative abundance of metazoan sequences in summer was higher than in other seasons (Figure S4). Therefore, the changes in the α diversity index and absolute abundance do not simply indicate an increase in species number, but rather a structural transformation characterized by a decline in community dominance and an increase in species evenness.

The variation in nutrients is also a key factor determining the seasonal changes of phytoplankton [4]. The upwelling along the coast in spring drives a large influx of phosphate (PO_4^{3-}), and transforms the Qiongdong region from a phosphorus-limited state in winter to a nitrogen-limited state in spring. At the same time, the relative abundance of Bacillariophyta reaches its highest point throughout the year. Nutrient changes may alter the seasonal variation pattern of phytoplankton functional traits, forming a trade-off between small-cell fast-growing species and large-cell species based on different strategies [45]. Studies have shown that Bacillariophyta are sensitive to changes in nutrient concentrations such as nitrogen and phosphorus [4,46], and especially when phosphorus concentrations increase, Bacillariophyta (diatom) abundance significantly increases, and they are more likely to form dominant groups [40]. Therefore, the seasonal dominance of Bacillariophyta in spring may reflect the regulatory effect of nutrient input on community structure under the influence of seasonal temperature fluctuations. Together, seasonal temperature and nutrient dynamics jointly shape the seasonal succession and functional structure of phytoplankton communities in the Qiongdong region.

4.3. Seasonal Restructuring of Phytoplankton MENs

Changes in communities are not only reflected in changes in species composition, but also in the adjustment of potential interactions between species, which is ultimately reflected in changes in the structure of MENs [9,47]. Although temperature affects all levels of eukaryotic communities and has a profound impact on the complexity and stability of networks [11], the results of its influence on network complexity in different ecosystems are inconsistent [11,48,49]. In the study area, the complexity of the network did not show a simple linear trend with temperature changes, but instead experienced a distinct network contraction in spring. During this period, the number of nodes, edges, and key nodes in the network all dropped to the lowest levels of the year, while the network's vulnerability reached its peak, indicating that the network structure was most fragile at this stage.

The network contraction in spring can be attributed to the alteration of the nutrient structure. Nutrients may reshape the relative advantages between different functional groups by changing the resource limitation state [40,50,51]. The upwelling in spring brings in the input of nutrients (with a significant increase in phosphate and $N/P < 16$), which alters the nutritional limitation status of the microbial community. This may have promoted the excessive proliferation of opportunistic R-strategy groups. Although this eutrophication stimulated the rapid accumulation of microbial biomass in the initial stage, it might have weakened the resilience of the community by promoting the growth of opportunistic groups (R-strategy) [52]. Specifically, a few fast-growing R-strategists quickly dominated the ecological niches, leading to a decrease in the aggregation and connectivity among the remaining community members, ultimately resulting in the observed simplification of the network topology [53]. Similarly, in the East China Sea, it has been observed that the complexity of the phytoplankton network in nutrient-replete areas is usually lower than that in nutrient-deficient areas [9]. In addition, research has indicated that under the background of rising temperatures and high phosphorus content, ecological networks typically exhibit reduced connectivity and weakened structural complexity [54]. Therefore, the lowest complexity of the spring network in this study likely reflects a temporary reorganization of

community interaction relationships under the combined effect of seasonal temperature and nutritional structure changes.

Furthermore, our data indicate that as the seasonal temperature rises, the overall robustness of the network declines, and the network's ability to resist interference in summer is significantly weaker than in winter. Although the complexity of the summer network has somewhat recovered compared to spring, the nature of the interactions has changed, with an increase in the proportion of negative correlations indicating an intensification of competitive exclusion or spatial isolation [55]. The mutual interaction within the community gradually shifts from cooperation to competition. The summer network does not simply revert to the complex state of winter but forms a new yet relatively fragile structure under environmental constraints. These findings emphasize that assessing ecosystem health based solely on biodiversity indices (which increased in summer) might overlook critical weaknesses in the underlying ecological fabric (the weakened network).

4.4. Community Assembly Processes Underlying Seasonal Network Dynamics

To further explain the mechanisms underlying the observed seasonal variation in network structure, we examined the community assembly processes of phytoplankton in the Qiongdong region. It is generally believed that community assembly processes are mainly influenced by deterministic processes at medium spatial scales or under conditions with significant environmental heterogeneity [56]. However, in this study, we first used NCM to assess the impact of stochasticity. The consistently high goodness-of-fit ($R^2 > 0.65$) across all three seasons indicates that the composition of the phytoplankton community in the Qiongdong region is mainly governed by stochastic processes rather than deterministic environmental filtering. Similarly, the iCAMP model also confirmed this view, with stochastic processes accounting for more than 50% in all three seasons.

One point to be noted in the iCAMP model is the seasonal fluctuation of dispersal limitation. Dispersal limitation refers to the restriction on the movement and settlement of individuals in new locations [57]. Our data show that the proportion of dispersal limitation increases in spring, and the migration rate in the NCM decreases during this period, indicating that the effect of dispersal limitation intensifies at this time. Therefore, the community turnover of phytoplankton may be more susceptible to local environmental factors, especially changes in nutrient limitations. Notably, although homogeneous selection in deterministic processes accounts for a relatively high proportion (>44%), it remains relatively stable across seasons, suggesting that the reorganization of the ecological network in spring may be driven by the intensification of dispersal limitation. Moreover, this intensification of dispersal limitation is consistent with the observed contraction and increased vulnerability of the molecular ecological network. High dispersal limitation restricts the movement of species within the region, and limited biological exchange between local communities leads to the differentiation of ecological community composition due to random changes in local population size [58], thereby resulting in the simplification of the molecular ecological network structure and a reduction in the overall stability of the system. This indicates that, although the overall contribution of the stochastic process remained relatively stable in spring, profound adjustments occurred within its internal components, with dispersal limitation replacing other processes to become the main force driving community assembly. Therefore, the enhanced dispersal limitation resulting from changes in the nutritional structure may weaken species dispersal and niche complementarity at the regional scale, ultimately leading to a reduction in the complexity of the molecular ecological network and a decrease in its stability.

5. Conclusions

This study provides a comprehensive mechanistic framework for understanding how seasonal environmental gradients shape phytoplankton community structure and ecological network stability in the Qiongdong region. Our results demonstrate that water temperature is a key factor influencing the seasonal succession of the community, while the input of nutrients brought by the upwelling in spring—especially the shift from phosphorus limitation to nitrogen limitation—plays a key role in reshaping the structure of the ecological network. A significant finding is the marked seasonal decoupling between biodiversity and network complexity. While α-diversity increases under warmer conditions, network complexity drops to its lowest in spring, forming a distinct network contraction and enhanced vulnerability. Mechanistically, this decoupling is mainly regulated by the transformation of community assembly processes. The alteration of the structure of nutrients may have intensified the dispersal limitation, thereby restricting species exchange at the regional scale, weakening the connectivity of interspecific interactions, and ultimately leading to the simplification of the network structure and the decline of system robustness. This result highlights the crucial but often overlooked role of dispersal limitation in linking environmental changes to the stability of ecological networks. However, this study is based on only three independent sampling periods, and the limited temporal resolution may not cover short-term random fluctuations or multi-year changes. Future studies with higher frequency monitoring are crucial for further validating these seasonal patterns. From a broader perspective, our findings imply that during seasonal environmental transitions, the interplay between temperature and nutrient availability may amplify ecosystem vulnerability by altering community assembly dynamics rather than merely changing species composition. This highlights the limitations of relying solely on biodiversity indicators to assess the health of ecosystems. Overall, this study advances our understanding of how environmental gradients translate into ecological instability and provides new insights into the mechanisms governing the resilience of coastal marine ecosystems.

Supplementary Materials: The following supporting information can be downloaded at https://www.mdpi.com/article/10.3390/jmse14080704/s1. Figure S1: Linear regression relationship between temperature and NMDS axes; Figure S2: Bar chart of gene-copy-based proxy for absolute phytoplankton abundance. QD2: winter; QD5: spring; QD8: summer; Figure S3: Box plots of α diversity indices, including Richness, Shannon index, Simpson index, and Pielou evenness index. The box represents the interquartile range, the middle line represents the median, and the whiskers represent the minimum and maximum values. QD2: winter; QD5: spring; QD8: summer. One-way ANOVA was used to test the differences among different seasons. NS indicates no significant difference, * $p < 0.05$, ** $p < 0.01$, *** $p < 0.001$; Figure S4: The relative content of Metazoa_Animalia in three seasons; Table S1: Comparison of the differences in phytoplankton community structure among three seasons based on ANOSIM.

Author Contributions: Conceptualization, G.J.; formal analysis, H.S.; investigation, H.S.; resources, J.C., H.S., and F.C.; data curation, H.S.; writing—original draft preparation, H.S.; writing—review and editing, G.J., H.S., and P.W.; visualization, H.S.; supervision, G.J.; project administration, G.J.; funding acquisition, G.J. All authors have read and agreed to the published version of the manuscript.

Funding: This study was funded by the National Natural Science Foundation of China (Grant 42030504) and was supported by the Southern Marine Science and Engineering Guangdong Laboratory (Zhuhai) (SML2024SP022, SML2024SP002).

Data Availability Statement: The data presented in this study are available on request from the corresponding author.

Acknowledgments: We thank Dongping Li, Zhongyuan Luo, Man Zhao, Ke Dong, Anqing Wang, Mengru Wang, Qiyao Zhao, and Hui Zeng for their help in sample collections.

Conflicts of Interest: The authors declare no conflicts of interest.

References

1. Cerfonteyn, M.; Groben, R.; Vaulot, D.; Gudmundsson, K.; Vannier, P.; Perez-Hernandez, M.D.; Marteinsson, V.P. The distribution and diversity of eukaryotic phytoplankton in the Icelandic marine environment. *Sci. Rep.* **2023**, *13*, 8519. [CrossRef] [PubMed]
2. Ma, W.T.; Chai, F.; Xiu, P.; Xue, H.J.; Tian, J. Modeling the long-term variability of phytoplankton functional groups and primary productivity in the South China Sea. *J. Oceanogr.* **2013**, *69*, 527–544. [CrossRef]
3. Chen, Z.; Sun, J.; Chen, D.W.; Wang, S.H.; Yu, H.; Chen, H.T.; Wang, M. Effects of Ocean Currents in the Western Pacific Ocean on Net-Phytoplankton Community Compositions. *Diversity* **2021**, *13*, 428. [CrossRef]
4. Wei, Y.Q.; Luan, Q.S.; Shan, X.J.; Cui, H.W.; Qu, K.M.; Cui, Z.G.; Sun, J. Temperature and nutrients drive distinct successions between diatoms and dinoflagellates over the past 40 years: Implications for climate warming and eutrophication. *Sci. Total Environ.* **2024**, *931*, 172997. [CrossRef]
5. Xiao, Y.Y.; Xu, Y.W.; Su, L.; Cai, Y.C.; Qi, Z.H.; Liu, Y.; Chen, Z.Z.; Lakshmikandan, M. Effects of seasonal variations and environmental factors on phytoplankton community structure and abundance in Beibu Gulf, China. *Ocean Coast. Manag.* **2024**, *248*, 106982. [CrossRef]
6. Wang, Y.Z.; Liu, Y.; Chen, X.Y.; Cui, Z.G.; Qu, K.M.; Wei, Y.Q. Exploring the key factors affecting the seasonal variation of phytoplankton in the coastal Yellow Sea. *Front. Mar. Sci.* **2022**, *9*, 1076975. [CrossRef]
7. Wu, J.; Zhu, Z.; Waniek, J.J.; Niu, M.; Wang, Y.; Zhang, Z.; Zhou, M.; Zhang, R. The biogeography and co-occurrence network patterns of bacteria and microeukaryotes in the estuarine and coastal waters. *Mar. Environ. Res.* **2023**, *184*, 105873. [CrossRef]
8. Liu, Q.; Li, Y.; Wang, H.; Yang, G.; Kan, J.; Yang, M.; Yu, X.; Guo, C.; Wang, M.; Wang, W.; et al. Assembly and Network Stability of Planktonic Microorganisms under the Influence of Salinity Gradient: An Arctic Case Study from the Lena River Estuary to the Laptev Sea. *Microbiol. Spectr.* **2023**, *11*, e02115-22. [CrossRef]
9. Lei, Z.Y.; Zhang, C.L.; He, L.; Xie, W. Different phytoplankton distributions and assembly processes in marine water masses with contrasting nutrient conditions. *BMC Microbiol.* **2025**, *25*, 105657. [CrossRef]
10. Zheng, X.; Wang, M.; Liu, X.; Xu, S.; Ma, S.; Wang, J.; Wang, C.; Zhan, A.; Yu, P.; Wang, D.; et al. Revealing assembly mechanisms of algal communities in aquatic microniches: Shifts in diversity patterns, microbial interactions and stability along nutrient gradients. *Environ. Res.* **2024**, *262*, 119798. [CrossRef]
11. Yu, S.; Cao, X.; Chen, P.; Liu, Y.; Duan, G.; Qi, W.; Peng, J.; Liu, H.; Qu, J. Climate warming and nutrient enrichment destabilize plankton network stability over the past century. *Commun. Earth Environ.* **2025**, *6*, 247. [CrossRef]
12. Li, K.H.; Lin, J.Q.; Wang, X.X.; Chen, T.; Liu, W.H. Stochastic process shapes the spatiotemporal patterns of main eukaryotic communities in a subtropical estuary. *Environ. Res.* **2025**, *285*, 122565. [CrossRef] [PubMed]
13. Zou, J.; Xiao, Y.; Wu, P.; Wang, T.; Lin, L.; Liu, Y.; Liu, Y.; Li, C. Distribution, community structure and assembly patterns of phytoplankton in the northern South China Sea. *Front. Microbiol.* **2024**, *15*, 1450706. [CrossRef] [PubMed]
14. Morales, S.E.; Tobias-Huenefeldt, S.P.; Armstrong, E.; Pearman, W.S.; Bogdanov, K. Marine phytoplankton impose strong selective pressures on in vitro microbiome assembly, but drift is the dominant process. *ISME Commun.* **2025**, *5*, ycaf001. [CrossRef] [PubMed]
15. Shao, Y.; Stewart, K.A.; Gsell, A.S.; Wang, S.; Xie, B.; Lin, H.; Geng, Z.; Yan, Z. Connecting diversity and process: Eukaryotic phytoplankton community dynamics across the Yangtze River using environmental DNA. *Ecol. Indic.* **2025**, *17*, 114026. [CrossRef]
16. Jiao, S.; Yang, Y.; Xu, Y.; Zhang, J.; Lu, Y. Balance between community assembly processes mediates species coexistence in agricultural soil microbiomes across eastern China. *ISME J.* **2020**, *14*, 202–216. [CrossRef]
17. Zheng, P.; Mao, A.; Meng, S.; Yu, F.; Zhang, S.; Lun, J.; Li, J.; Hu, Z. Assembly mechanism of microbial community under different seasons in Shantou sea area. *Mar. Pollut. Bull.* **2024**, *205*, 116550. [CrossRef]
18. Wang, H.; Wu, Z.; Zhao, A.; Wang, Y.; Li, Q.; Zhang, L.; Wang, Z.; Li, T.; Zhao, J. Distinct patterns and processes of eukaryotic phytoplankton communities along a steep elevational gradient in highland rivers. *Environ. Res.* **2025**, *275*, 121427. [CrossRef]
19. Li, K.; Yin, J.; Huang, L.; Zhang, J.; Lian, S.; Liu, C. Distribution and abundance of thaliaceans in the northwest continental shelf of South China Sea, with response to environmental factors driven by monsoon. *Cont. Shelf Res.* **2011**, *31*, 979–989. [CrossRef]
20. Liu, T.; Li, S.; Hou, H.; Li, Y.; Yang, B.; Sun, W.; Wang, G.; Liang, G.; Teng, F. Seasonal and interannual variation characteristics of Qiongdong thermal front. *Mar. Sci.* **2024**, *48*, 13–26.
21. Liu, X.; Xie, N.; Bai, M.; Li, J.; Wang, G. Composition change and decreased diversity of microbial eukaryotes in the coastal upwelling waters of South China Sea. *Sci. Total Environ.* **2021**, *795*, 148892. [CrossRef] [PubMed]
22. Tong, Z.; Jiao, J.; Xiao, W.; Zhou, K.; Huang, B. Bottom-Up Control and Phytoplankton Succession in a Subtropical Upwelling System. *J. Geophys. Res. Ocean.* **2025**, *130*, e2025JC022413. [CrossRef]
23. Salmaso, N.; Boscaini, A.; Pindo, M. Unraveling the Diversity of Eukaryotic Microplankton in a Large and Deep Perialpine Lake Using a High Throughput Sequencing Approach. *Front. Microbiol.* **2020**, *11*, 789. [CrossRef] [PubMed]

24. Chen, S.F.; Zhou, Y.Q.; Chen, Y.R.; Gu, J. fastp: An ultra-fast all-in-one FASTQ preprocessor. *Bioinformatics* **2018**, *34*, i884–i890. [CrossRef]
25. Callahan, B.J.; McMurdie, P.J.; Rosen, M.J.; Han, A.W.; Johnson, A.J.A.; Holmes, S.P. DADA2: High-resolution sample inference from Illumina amplicon data. *Nat. Methods* **2016**, *13*, 581–583. [CrossRef]
26. Quast, C.; Pruesse, E.; Yilmaz, P.; Gerken, J.; Schweer, T.; Yarza, P.; Peplies, J.; Gloeckner, F.O. The SILVA ribosomal RNA gene database project: Improved data processing and web-based tools. *Nucleic Acids Res.* **2013**, *41*, D590–D596. [CrossRef]
27. Song, L.; Wu, J.; Du, J.; Li, N.; Song, G.J.; Wang, K.; Sun, M.; Wang, P. The Characteristics and Distribution of Eukaryotic Phytoplankton Community in Liaodong Bay, China. *Ocean Sci. J.* **2019**, *54*, 183–203. [CrossRef]
28. Tettamanti Boshier, F.A.; Srinivasan, S.; Lopez, A.; Hoffman, N.G.; Proll, S.; Fredricks, D.N.; Schiffer, J.T. Complementing 16S rRNA Gene Amplicon Sequencing with Total Bacterial Load To Infer Absolute Species Concentrations in the Vaginal Microbiome. *mSystems* **2020**, *5*, 2. [CrossRef]
29. Jiang, H.; Chen, Y.; Hu, Y.; Wang, Z.; Lu, X. Soil Bacterial Communities and Diversity in Alpine Grasslands on the Tibetan Plateau Based on 16S rRNA Gene Sequencing. *Front. Ecol. Evol.* **2021**, *9*, 630722. [CrossRef]
30. Liu, S.Y.; Cui, Z.M.; Zhao, Y.F.; Chen, N.S. Composition and spatial-temporal dynamics of phytoplankton community shaped by environmental selection and interactions in the Jiaozhou Bay. *Water Res.* **2022**, *218*, 118488. [CrossRef]
31. Feng, K.; Peng, X.; Zhang, Z.; Gu, S.S.; He, Q.; Shen, W.L.; Wang, Z.J.; Wang, D.R.; Hu, Q.L.; Li, Y.; et al. iNAP: An integrated network analysis pipeline for microbiome studies. *iMeta* **2022**, *1*, e13. [CrossRef] [PubMed]
32. Zhang, L.; Zhang, H.; Liu, H.; Wu, W.; Xu, Z.; Tan, Y.; Shi, Z.; Xia, X. Phosphorus availability shapes size structure, co-occurrence patterns and network stability of surface microeukaryotic plankton communities in an urbanized estuarine ecosystem. *Ecol. Indic.* **2023**, *154*, 110548. [CrossRef]
33. Sloan, W.T.; Lunn, M.; Woodcock, S.; Head, I.M.; Nee, S.; Curtis, T.P. Quantifying the roles of immigration and chance in shaping prokaryote community structure. *Environ. Microbiol.* **2006**, *8*, 732–740. [CrossRef] [PubMed]
34. Ning, D.L.; Yuan, M.T.; Wu, L.W.; Zhang, Y.; Guo, X.; Zhou, X.S.; Yang, Y.F.; Arkin, A.P.; Firestone, M.K.; Zhou, J.Z. A quantitative framework reveals ecological drivers of grassland microbial community assembly in response to warming. *Nat. Commun.* **2020**, *11*, 4717. [CrossRef]
35. Cheng, L.J.; Li, G.C.; Long, S.M.; Li, Y.L.; von Schuckmann, K.; Trenberth, K.E.; Mann, M.E.; Abraham, J.; Du, Y.; Cheng, X.H.; et al. Ocean stratification in a warming climate. *Nat. Rev. Earth Environ.* **2025**, *6*, 637–655. [CrossRef]
36. Andersen, I.M.; Taylor, J.M.; Graeber, D.; Kelly, P.T.; Hoke, A.K.; Robbins, C.J.; Scott, J.T. Redfield revisited: Insights into freshwater seston carbon : Nitrogen : Phosphorus stoichiometry. *Limnol. Oceanogr.* **2025**, *70*, S14–S26. [CrossRef]
37. Kim, T.-H.; Kim, G. Changes in seawater N:P ratios in the northwestern Pacific Ocean in response to increasing atmospheric N deposition: Results from the East (Japan) Sea. *Limnol. Oceanogr.* **2013**, *58*, 1907–1914. [CrossRef]
38. Shaw, P.T.; Chao, S.Y. Surface circulation in the South China Sea. *Deep Sea Res. Part I Oceanogr. Res. Pap.* **1994**, *41*, 1663–1683. [CrossRef]
39. Chen, T.T.; Zhang, Y.X.; Song, S.Q.; Liu, Y.; Sun, X.X.; Li, C.W. Diversity and seasonal variation of marine phytoplankton in Jiaozhou Bay, China revealed by morphological observation and metabarcoding. *J. Oceanol. Limnol.* **2022**, *40*, 577–591. [CrossRef]
40. Fu, X.T.; Shi, W.T.; Liu, Z.S.; Wang, X.Z.; Zhang, G.C.; Sun, J. Impact of environmental variables on the distribution of phytoplankton communities in the Southern Yellow Sea. *Environ. Res.* **2024**, *243*, 117862. [CrossRef]
41. Sherman, E.; Moore, J.K.; Primeau, F.; Tanouye, D. Temperature influence on phytoplankton community growth rates. *Glob. Biogeochem. Cycles* **2016**, *30*, 550–559. [CrossRef]
42. Gerhard, M.; Schlenker, A.; Hillebrand, H.; Striebel, M. Environmental stoichiometry mediates phytoplankton diversity effects on communities' resource use efficiency and biomass. *J. Ecol.* **2022**, *110*, 430–442. [CrossRef]
43. Ji, L.; Zhang, H.Y.; Wang, Z.Y.; Tian, Y.L.; Tian, W.; Liu, Z. Temperature orchestrates phytoplankton community and environment in mountain stream for enhancing resource use efficiency. *Front. Mar. Sci.* **2025**, *12*, 1565858. [CrossRef]
44. Lewandowska, A.M.; Hillebrand, H.; Lengfellner, K.; Sommer, U. Temperature effects on phytoplankton diversity—The zooplankton link. *J. Sea Res.* **2014**, *85*, 359–364. [CrossRef]
45. Wentzky, V.C.; Tittel, J.; Jäger, C.G.; Bruggeman, J.; Rinke, K. Seasonal succession of functional traits in phytoplankton communities and their interaction with trophic state. *J. Ecol.* **2020**, *108*, 1649–1663. [CrossRef]
46. Smucker, N.J.; Pilgrim, E.M.; Nietch, C.T.; Darling, J.A.; Johnson, B.R. DNA metabarcoding effectively quantifies diatom responses to nutrients in streams. *Ecol. Appl.* **2020**, *30*, 550–559. [CrossRef]
47. Zhu, C.Y.; Liu, W.W.; Li, X.H.; Xu, Y.S.; El-Serehy, H.A.; Al-Farraj, S.A.; Ma, H.G.; Stoeck, T.; Yi, Z.Z. High salinity gradients and intermediate spatial scales shaped similar biogeographical and co-occurrence patterns of microeukaryotes in a tropical freshwater-saltwater ecosystem. *Environ. Microbiol.* **2021**, *23*, 4778–4796. [CrossRef]
48. Chen, C.Z.; Li, P.; Yin, M.H.; Wang, J.X.; Sun, Y.J.; Ju, W.M.; Liu, L.; Li, Z.H. Deciphering characterization of seasonal variations in microbial communities of marine ranching: Diversity, co-occurrence network patterns, and assembly processes. *Mar. Pollut. Bull.* **2023**, *197*, 115739. [CrossRef]

49. Hou, D.D.; Yan, H.Z.; Lin, H.Y.; Zhang, H.J.; Zhang, D.M.; Wang, K. Biogeographic shifts in the microbial co-occurrence network features of three domains across complex environmental gradients in subtropical coastal waters. *Ecol. Process.* **2024**, *13*, 74. [CrossRef]
50. Wu, P.-F.; Li, D.-X.; Kong, L.-F.; Li, Y.-Y.; Zhang, H.; Xie, Z.-X.; Lin, L.; Wang, D.-Z. The diversity and biogeography of microeukaryotes in the euphotic zone of the northwestern Pacific Ocean. *Sci. Total Environ.* **2020**, *698*, 134289. [CrossRef]
51. Xiao, W.P.; Liu, X.; Irwin, A.J.; Laws, E.A.; Wang, L.; Chen, B.Z.; Zeng, Y.; Huang, B.Q. Warming and eutrophication combine to restructure diatoms and dinoflagellates. *Water Res.* **2018**, *128*, 206–216. [CrossRef]
52. Li, H.; Fu, J.; Fan, X.; He, Z.; Wang, Y.; Yang, S.; Wu, J.; Wu, L.; Zhou, J. Eutrophication Reshapes Microbial Communities and Life-History Strategies in the Riverine Ecosystems. *Environ. Microbiol. Rep.* **2025**, *17*, e70234. [CrossRef] [PubMed]
53. Wang, Y.; Qu, M.; Wang, J.; Zhu, W.; Li, J. Recovery of bacterial network complexity and stability after simulated extreme rainfall is mediated by K- /r-strategy dominance. *Appl. Soil Ecol.* **2024**, *203*, 105657. [CrossRef]
54. Merz, E.; Saberski, E.; Gilarranz, L.J.; Isles, P.D.F.; Sugihara, G.; Berger, C.; Pomati, F. Disruption of ecological networks in lakes by climate change and nutrient fluctuations. *Nat. Clim. Change* **2023**, *13*, 389–396. [CrossRef] [PubMed]
55. Yuan, M.M.; Guo, X.; Wu, L.; Zhang, Y.; Xiao, N.; Ning, D.; Shi, Z.; Zhou, X.; Wu, L.; Yang, Y.; et al. Climate warming enhances microbial network complexity and stability. *Nat. Clim. Change* **2021**, *11*, 343–348. [CrossRef]
56. Li, T.C.; Liu, G.L.; Yuan, H.T.; Chen, J.W.; Lin, X.; Li, H.F.; Yu, L.Y.; Wang, C.; Li, L.; Zhuang, Y.Y.; et al. Eukaryotic plankton community assembly and influencing factors between continental shelf and slope sites in the northern South China Sea. *Environ. Res.* **2023**, *216*, 114584. [CrossRef]
57. Zhu, A.; Liang, Z.; Gao, L.; Xie, Z. Dispersal limitation determines the ecological processes that regulate the seasonal assembly of bacterial communities in a subtropical river. *Front. Microbiol.* **2024**, *15*, 1430073. [CrossRef]
58. Stegen, J.C.; Lin, X.; Fredrickson, J.K.; Chen, X.; Kennedy, D.W.; Murray, C.J.; Rockhold, M.L.; Konopka, A. Quantifying community assembly processes and identifying features that impose them. *ISME J.* **2013**, *7*, 2069–2079. [CrossRef]

Disclaimer/Publisher's Note: The statements, opinions and data contained in all publications are solely those of the individual author(s) and contributor(s) and not of MDPI and/or the editor(s). MDPI and/or the editor(s) disclaim responsibility for any injury to people or property resulting from any ideas, methods, instructions or products referred to in the content.